Physics – Uspekhi **60** (9) 931 – 934 (2017)

FROM THE CURRENT LITERATURE

PACS numbers: 02.60.Cb, **05.45. – a**, **45.40. – f**

Retrograde motion of a rolling disk

A V Borisov, A A Kilin, Yu L Karavaev

DOI: https://doi.org/10.3367/UFNe.2017.01.038049

Abstract. This paper presents results of theoretical and experimental research explaining the retrograde final-stage rolling of a disk under certain relations between its mass and geometric parameters. Modifying the no-slip model of a rolling disk by including viscous rolling friction provides a qualitative explanation for the disk's retrograde motion. At the same time, the simple experiments described in the paper completely reject the aerodynamical drag torque as a key reason for the retrograde motion of a disk considered, thus disproving some recent hypotheses.

Keywords: retrograde turn, rolling disk, nonholonomic model, rolling friction

The authors of Ref. [1] brought out an intuitively nontrivial fact — the turn of a rolling disk with a central hole. Invoking an analogy with planetary motion in celestial mechanics, they designated such motion 'retrograde'. It should be recalled that in the Russian literature [2] the term used to denote motion like this one is referred to as 'backward', whereas the term implying the opposite is 'forward'. Using 'backward' and 'forward' to describe the rolling of a disk hides the physical sense of motion, so that the English terminology of 'retrograde' and 'prograde' motions will be used below to describe the main disk motions, respectively, in opposition to and along a disk's rotation.

In the opinion of the authors of Ref. [1], the turn is caused by aerodynamical drag forces arising because of the presence of the central hole in the disk. However, the model proposed by them does not reflect the physical nature of the disk rolling process. Similar concerns (see Refs [3–5]) were raised with respect to the work by Moffat [6], who considered aerodynamical drag as the basic mechanism dissipating the energy of a homogeneous disk. Nevertheless, it revived interest in exploring spinning disk dynamics and triggered a large number of papers, whose results cannot be ignored if one seeks a description of the retrograde turn of a disk with a central hole, sometimes called a ring (especially when the hole diameter tends to that of the disk).

The bibliography of work exploring the problem of solid disk motion, also known as Euler's disk problem, can be found in Refs [7–12]. There are two models describing Euler's disk dynamics, which account for its contact with the surface: one without slip [13], and the other one with slip [4, 14]. Note that slip is observed in experiments through initial motion stages, being subsequently replaced by rolling. The question of applicability of different models for contact interaction is also discussed in relation to the rolling of a hollow cylinder [15]. It should be remembered that models with idealized slip are described by Hamiltonian systems, whereas models with idealized rolling are described by nonholonomic systems. Euler's disk dynamics received extensive treatment for various models of friction, and yet some questions still remain open (for example, disk shudder before the disk comes to rest [11]).

As follows from experiments, the rolling trajectory of a spinning homogeneous disk differs from that of a spinning ring by the absence of the turn, and represents a wavy spiral. Based on theoretical and numerical studies [13], we have shown that both retrograde and prograde disk rolling can be observed in a nonholonomic model for certain mass-geometric characteristics, being a function of the energy level. However, the framework of the nonholonomic model does not allow transitions between energy levels.

It should be mentioned that the ring turn effect discovered by the authors of Ref. [1] is neither new nor solely related to rings. It was reported in earlier studies by A C Or, who carried out numerical simulations of the Thompson top [16], and in the recent experimental work of R Cross [17]. The aerodynamics of the tops explored in these studies is substantially different from ring dynamics.

The disproof of the thesis that aerodynamical drag is the main cause of the turn of a spinning ring may rely on simple experiments that we carried out. For the first experiment (see movie 1 [18]) we made a special ring with the central hole of a cylindrical shape with a radius of 33 mm, whereas the upper and lower rims of the ring had different radii $R_1 = 40$ mm and $R_2 = 35$ mm (i.e., the ring in its diametral section looks likes an isosceles trapezoid). If the ring rolls on its large rim, its trajectory of motion resembles that of a disk and does not exhibit retrograde motions; however, the ring performs a retrograde turn if it rolls on its smaller rim independent of initial conditions. The angular momenta of aerodynamic drag differ but slightly when the ring rolls on its large or small rims, and yet the motion character differs dramatically. The results of this experiment allow a conclusion to be drawn that the

A V Borisov Moscow Institute of Physics and Technology (State University),
Institutskii per. 9, 141700 Dolgoprudnyi, Moscow region, Russian Federation;
National Research Nuclear University MEPhI,
Kashirskoe shosse 31, 115409 Moscow, Russian Federation
E-mail: borisov@rcd.ru
A A Kilin Udmurt State University,
ul. Universitetskaya 1, 426034 Izhevsk, Russian Federation
E-mail: aka@rcd.ru
Yu L Karavaev Udmurt State University,
ul. Universitetskaya 1, 426034 Izhevsk, Russian Federation;
M T Kalashnikov Izhevsk State Technical University,
ul. Studencheskaya 7, 426069 Izhevsk, Russian Federation
E-mail: karavaev_yury@istu.ru

Received 1 December 2016, revised 10 January 2017
Uspekhi Fizicheskikh Nauk **187** (9) 1003 – 1006 (2017)
DOI: https://doi.org/10.3367/UFNr.2017.01.038049
Translated by S D Danilov; edited by A Radzig

presence of retrograde ring turn is strongly dependent on the relationship between the ring radius of inertia and the radius of the rim the ring rolls on.

As a continuation of this experiment, we sealed up one of the ring surfaces with an adhesive film (see movie 2 [19]); the mass-inertia properties of the ring were largely unaffected by this intervention, but the ring aerodynamics became nearly those of the disk. The results were similar to those of the previous experiment: when rolling on its smaller rim, the ring performed a retrograde turn, and this did not occur when the ring rolled on the larger rim. Similar experiments were conducted with rings having different geometrical and mass characteristics. The independence of ring trajectories from the film presence invites the conclusion that air resistance affects the dynamics of ring rolling only weakly.

The third experiment was carried out in a vacuum chamber used for casting. The pressure in the chamber was lowered to 10^2 Pa (0.0145 psi [1]). Experiments were performed with a usual wedding ring made of gold, which was thrown on an aluminum plate with the help of driving mechanisms installed in the vacuum chamber. The retrograde ring turn effect was preserved in the vacuum chamber, as demonstrated by movies [20, 12]. These experiments allow us to unequivocally rule out aerodynamic forces from the basic factors leading to the retrograde ring turn.

In our opinion, to describe retrograde motion dynamics, it is convenient to use a modified nonholonomic model of a disk rolling [13] that takes into account the rolling friction. This model also describes the ring dynamics, which differ from those of a disk only through the mass-geometric parameters. The practice of modifying idealized models proved to be efficient for explaining the qualitative effects in some problems, e.g., in cases regarding the Thomson top [17] or rattleback [22]. Despite substantial disparity between experimental and theoretical data, the modified models can serve as a simple tool to qualitatively explain phenomena accompanying the motion of physical bodies.

The nonholonomic model allows both prograde and retrograde trajectories in a disk motion [13]. The addition of dissipation to the nonholonomic model would provide a transition from prograde rolling to a retrograde turn. Dissipation in this case can be described by various models. The most thorough results of exploring the mechanisms of spinning disk energy dissipation, including experimental ones, are presented in Refs [10, 23]. According to their authors, after a short stage of slip, the main factor affecting the dynamics of Euler's disk is the rolling friction, which is modelled in Refs [12, 23] as a viscous contact with a quadratic dependence on the motion velocity. This is confirmed by the rather good agreement between the results of numerical simulations for the nutation angle and the precession speed, and the experimental results. However, the authors of Refs [10, 23] did not pay necessary attention to the trajectories of disk motion in the framework of the explored friction models or to the dependence of the trajectory shape on mass-geometric characteristics of a disk. Notice that Contensou [24] was the first to construct the viscous contact model.

To describe the disk motion, we consider two reference frames (Fig. 1). The first one, $OXYZ$, is at rest, and its unit

[1] psi is an off-system unit of measure for pressure: pound-force per square inch: 1 psi = 6894.75729 Pa.

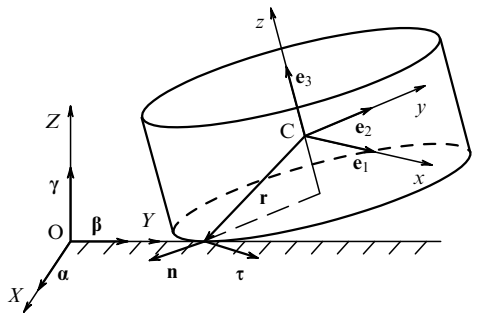

Figure 1. Disk rolling on a horizontal plane.

vectors are $\boldsymbol{\alpha}$, $\boldsymbol{\beta}$, $\boldsymbol{\gamma}$; the second one, $Cxyz$, is moving, being stiffly coupled to the disk center of mass, with the unit vectors $\mathbf{e}_1$, $\mathbf{e}_2$, $\mathbf{e}_3$. The position of the system will be specified through the coordinates of the disk center of mass in the fixed reference frame: $\mathbf{r}_c = (X, Y, Z)$ and the matrix $\mathbf{Q} = (\boldsymbol{\alpha}, \boldsymbol{\beta}, \boldsymbol{\gamma})$ describing the disk orientation in space. Here and in what follows (unless otherwise specified), all vectors are expressed in projections on the axes of the mowing reference frame $Cxyz$.

The equations of disk motion can be written down in the form

$$\mathbf{I}\dot{\boldsymbol{\omega}} = \mathbf{I}\boldsymbol{\omega} \times \boldsymbol{\omega} + \mathbf{r} \times \mathbf{N} + \mathbf{M}_f\,, \quad m\dot{\mathbf{v}} = m\mathbf{v} \times \boldsymbol{\omega} - mg\boldsymbol{\gamma} + \mathbf{N}\,. \tag{1}$$

Here, $\mathbf{M}_f$, $\mathbf{N}$ are, respectively, the torque of rolling friction and the plane reaction force, m is the disk mass, and $\mathbf{r}$ is the radius vector of the contact point in the moving reference frame:

$$\mathbf{r} = \left(-\frac{R\gamma_1}{\sqrt{1-\gamma_3{}^2}}\,, -\frac{R\gamma_2}{\sqrt{1-\gamma_3{}^2}}\,, -h \right), \tag{2}$$

where R is the radius of the rim the disk rolls on, h is the distance from this rim to the center of mass, and $\gamma_1, \gamma_2, \gamma_3$ are the components (directional cosines) of the vertical vector in the moving coordinate system.

The absence of slip at the contact point is provided by the nonholonomic constraint

$$\mathbf{f} = \mathbf{v} + \boldsymbol{\omega} \times \mathbf{r} = 0\,. \tag{3}$$

Solving the combination of equation (1) and the time derivative of constraint (3), one may find the reaction force $\mathbf{N}$. Inserting the expression obtained into the first equation (1) and eliminating the velocities with the help of constraint (3), we arrive at

$$\mathbf{I}\dot{\boldsymbol{\omega}} = \mathbf{I}\boldsymbol{\omega} \times \boldsymbol{\omega} + m\mathbf{r} \times \left(\mathbf{r} \times \dot{\boldsymbol{\omega}} + \dot{\mathbf{r}} \times \boldsymbol{\omega} - (\mathbf{r} \times \boldsymbol{\omega}) \times \boldsymbol{\omega} + g\boldsymbol{\gamma} \right) + \mathbf{M}_f\,. \tag{4}$$

Based on physical considerations, the torque of rolling friction can be factorized into three components that correspond to frictional torques in different directions (see also Ref. [23]): the torque opposing the disk rotation relative to the vertical $\boldsymbol{\gamma}$ with friction coefficient μ_γ, the torque opposing the turn of the disk around the vector $\boldsymbol{\tau}$ tangent to the disk rim at the point of contact with the surface with friction coefficient μ_τ, and the frictional torque opposing the disk rolling on its lower rim with friction coefficient μ_n. In general, when all three friction coefficients are distinct, the

frictional torque can be written down as

$$\mathbf{M}_{\mathrm{f}} = -\widehat{\boldsymbol{\mu}}\boldsymbol{\omega}, \quad \widehat{\boldsymbol{\mu}} = \mu_\gamma \boldsymbol{\gamma} \otimes \boldsymbol{\gamma} + \mu_\tau \boldsymbol{\tau} \otimes \boldsymbol{\tau} + \mu_n \mathbf{n} \otimes \mathbf{n}, \qquad (5)$$

where the unit tangent ($\boldsymbol{\tau}$) and normal ($\mathbf{n}$) vectors at the contact point are expressed as

$$\boldsymbol{\tau} = \frac{\boldsymbol{\gamma} \times \mathbf{e}_3}{\sqrt{1-\gamma_3{}^2}}, \quad \mathbf{n} = \frac{\boldsymbol{\gamma} \times (\mathbf{e}_3 \times \boldsymbol{\gamma})}{\sqrt{1-\gamma_3{}^2}},$$

and the tensor product of vectors $\mathbf{a}$, $\mathbf{b}$ is defined as follows;

$$\mathbf{a} \otimes \mathbf{b} = \|a_i b_j\|.$$

In general, the friction coefficient μ_γ, μ_τ, μ_n can depend on the phase variables and the reaction force $\mathbf{N}$ of a plane. In this paper, we limit ourselves to considering the case of viscous rolling friction, linear in angular velocities. In this case, the coefficients μ_γ, μ_τ, and μ_n are constant. Furthermore, to simplify the model, we assume that all three coefficients are equal: $\mu_\gamma = \mu_\tau = \mu_n = \mu$, and the rolling friction torque takes the form $\mathbf{M}_{\mathrm{f}} = -\mu\boldsymbol{\omega}$. It turns out that, even with such a notably rough assumption, the results of numerical modeling qualitatively agree with the experimental results.

Adding to equation (4) the kinematic Euler equations and quadratures for the disk center of mass, we obtain a closed system of equations describing the disk dynamics:

$$\mathbf{I}\dot{\boldsymbol{\omega}} + \boldsymbol{\omega} \times \mathbf{I}\boldsymbol{\omega} + m(\mathbf{r} \times \dot{\boldsymbol{\omega}} + \dot{\mathbf{r}} \times \boldsymbol{\omega} - (\mathbf{r} \times \boldsymbol{\omega}) \times \boldsymbol{\omega} + g\boldsymbol{\gamma}) \times \mathbf{r} = -\mu\boldsymbol{\omega}, \quad \dot{\boldsymbol{\alpha}} = \boldsymbol{\alpha} \times \boldsymbol{\omega}, \quad \dot{\boldsymbol{\beta}} = \boldsymbol{\beta} \times \boldsymbol{\omega}, \quad \dot{\boldsymbol{\gamma}} = \boldsymbol{\gamma} \times \boldsymbol{\omega},$$
$$\dot{x} = (\boldsymbol{\alpha}, \mathbf{r} \times \boldsymbol{\omega}), \quad \dot{y} = (\boldsymbol{\beta}, \mathbf{r} \times \boldsymbol{\omega}). \qquad (6)$$

Further, we present the results of numerical modeling of equations (6), comparing them with available experimental results.

To obtain quantitative experimental data on the motion trajectory, we developed a second experimental sample — a ring with variable radius (as a function of height), the diametral section of which is presented in Fig. 2a. The ring parameters are as follows: the radii of the rims $R_1 = 0.0375$ m and $R_2 = 0.0490$ m, the mass $m = 0.1034$, the moments of inertia about axes $I_x = I_y = 0.08647 \times 10^{-3}$ kg m^2 and $I_z = 0.16610 \times 10^{-3}$ kg m^2, the height of the center of mass $h = 0.0105$ m. The experimental trajectory of the center of mass was retrieved with the help of a motion tracking system working at the frequency of 200 Hz and referring to markers located on the ring (Fig. 2b).

Retrograde turns were not observed when the experimental sample rolled on its largest rim at different initial conditions. However, when it rolled on its smaller rim, retrograde turns were observed for those initial conditions which correspond to an energy level that exceeds some critical value. An example of the experimental trajectory of the ring rolling on its smaller rim is given in Fig. 3b.

With the help of the motion tracking system, the following initial conditions were obtained for a given trajectory: $\omega_1(0) = -2.5119$, $\omega_2(0) = 7.6737$, $\omega_3(0) = 29.2722$, and $\gamma_3 = 0.7175$, which were then utilized to carry out numerical modeling. The remaining initial conditions can be specified in an arbitrary way because of the axial disk symmetry and freedom in the choice of a fixed coordinate

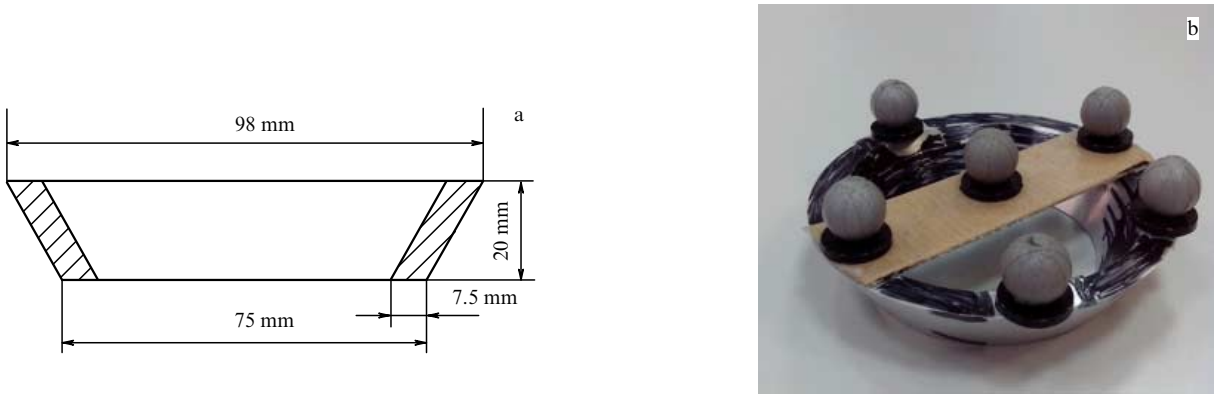

Figure 2. (a) Schematic of experimental sample; (b) photograph of experimental sample with the tracking system markers placed on it.

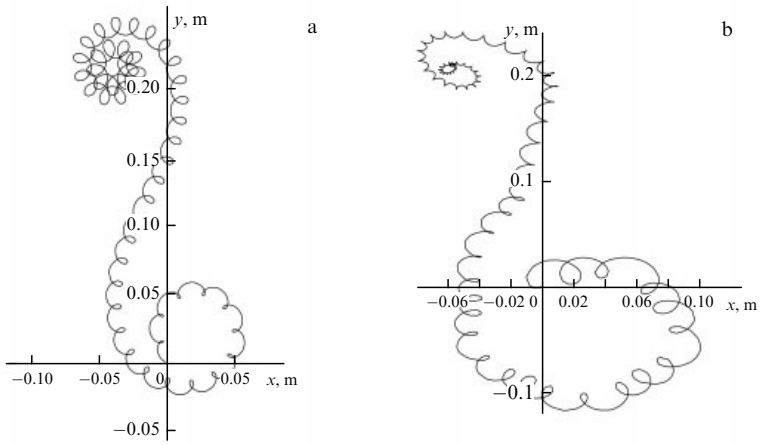

Figure 3. (a) Trajectory of a rolling ring with account for rolling friction (numerical simulations). (b) Trajectory of a rolling ring retrieved with the help of a motion tracking system.

system. The trajectory of a rolling ring obtained by numerically solving equations (6) for the initial conditions specified above and friction coefficient $\mu = 5.17 \times 10^{-6}$ is shown in Fig. 3a.

As is seen from Fig. 3, the shape of the trajectory is in qualitative agreement with the experimental results. The size and the number of loops on the trajectory strongly depend on the friction coefficient, and their consistency with experiment can be achieved by introducing a variable rolling friction into the model. The results of numerical modeling indicate that the solution of the system is sensitive to the initial conditions and magnitude of the friction coefficient. However, qualitatively, the character of the trajectory coincides with that obtained in experiments in the wide range of disk mass-geometric parameters and initial conditions.

In this article, we limited ourselves to considering only one model of viscous rolling friction, because the studies of dissipation mechanisms carried out in Refs [10, 23] indicated its key importance and good agreement with experiment. Nevertheless, we note that the retrograde turn discussed here was also experimentally observed in the case of rolling with slip that occurred on individual parts of a trajectory. When using a model in which the disk rolls with slip the entire time, a disk turn was not observed. However, the treatment of the model with slip at some sections of disk trajectory presents a more complicated task, because the transition from slip to rolling requires accounting for dry friction, which can lead to paradoxic phenomena [25, 26] and calls for special research. For this reason, the results have an unpredictable character on the level of a quantitative explanation and can hardly be obtained in the nearest future. To theoretically construct a trajectory that would quantitatively coincide with the experimental one seems impossible because of the presence of microroughness and the inhomogeneity of material characteristics, which is important in problems with friction.

To conclude, we briefly reiterate the results obtained in our work.

(1) Aerodynamical drag is not the main cause of the spinning ring turn.

(2) The phenomenon of ring turn can be qualitatively explained in the framework of disk rolling model without slip due to the presence of a viscous rolling friction.

(3) Because of randomness and the paradoxic character of transitions between the rolling and sliding frictions, which take place at certain sections of motion trajectory, the construction of ring motion trajectory that would quantitatively coincide with the experimental trajectory encounters difficulties.

Acknowledgments

The authors are indebted to I S Mamaev for fruitful discussions of the results obtained. The work was performed in the framework of the basic part of the State task to institutions of higher learning and also supported by RFBR grants (projects 15-08-09261-a and 15-38-20879 mol_a_ved).

References

1. Jalali M A, Sarebangholi M S, Alam M-R *Phys. Rev. E* **92** 032913 (2015)
2. Szebehely V *Theory of Orbits*: *the Restricted Problem of Three Bodies* (New York: Academic Press, 1967); Translated into Russian: *Teoriya Orbit*: *Ogranichennaya Zadacha Trekh Tel* (Moscow: Nauka, 1982)
3. Ruina A "Comments on Euler's disk and its finite-time singularity by H.K. Moffatt", Unpublished notes (Ithaca, NY: Dept. of Theoretical and Applied Mechanics, Cornell Univ., 2000)
4. Van den Engh G, Nelson P, Roach J *Nature* **408** 540 (2000)
5. Petrie D, Hunt J L, Gray C G *Am. J. Phys.* **70** 1025 (2002)
6. Moffatt H K *Nature* **404** 833 (2000)
7. Kessler P, O'Reilly O M *Regular Chaotic Dynamics* **7** 49 (2002)
8. Caps H et al. *Phys. Rev. E* **69** 056610 (2004)
9. Saje M, Zupan D *Multidiscipline Modeling Mater. Struct.* **2** 49 (2006)
10. Leine R L *Archive Appl. Mech.* **79** 1063 (2009)
11. Borisov A V, Mamaev I S, Karavaev Yu L *Nonlinear Dynamics* **79** 2287 (2015)
12. Ma D, Liu C *J. Appl. Mech.* **83** 061003 (2016)
13. Borisov A V, Mamaev I S, Kilin A A *Regular Chaotic Dynamics* **8** 201 (2003)
14. Przybylska M, Rauch-Wojciechowski S *Regular Chaotic Dynamics* **21** 204 (2016)
15. Srinivasan M, Ruina A *Phys. Rev. E* **78** 066609 (2008)
16. Or A C *SIAM J. Appl. Math.* **54** 597 (1994)
17. Cross R *Am. J. Phys.* **81** 280 (2013)
18. Karavaev Y L, Kilin A A, Borisov A V "The spinning motion of a ring, 2016", https://youtu.be/SEIyoQ0iWdI
19. Karavaev Y L, Kilin A A, Borisov A V "The spinning motion of a ring after applying adhesive film to it (2016)", https://youtu.be/l9C1KNq3OqU
20. Karavaev Y L, Kilin A A, Borisov A V "The spinning motion of a ring in a vacuum (2016)", https://youtu.be/VnktVz4H6R0
21. Karavaev Y L, Kilin A A, Borisov A V "The spinning motion of a ring at atmospheric pressure (2016)", https://youtu.be/s3SiPwxgoIk
22. Takano H *Regular Chaotic Dynamics* **19** 81 (2014)
23. Ma D, Liu C, Zhao Z, Zhang H *Proc. R. Soc. London A* **470** 20140191 (2014)
24. Contensou P, in *Kreiselprobleme Gyrodynamics, Intern. Union of Theoretical and Applied Mechanics Symp. Celerina, Switzerland, 1962* (Ed. H Ziegler) (Berlin: Springer, 1963) p. 201
25. Mamaev I S, Ivanova T B *Regular Chaotic Dynamics* **19** 116 (2014)
26. Ivanova T B, Mamaev I S *J. Appl. Math. Mech.* **80** 7 (2016); *Priklad. Mat. Mekh.* **80** 11 (2016)